A Scanning Technique to Measure Regional Cerebral Blood Flow and Oxyhemoglobin Level

Hiroyuki Nakase, M.D., Toshisuke Sakaki, M.D., Oliver Kempski, M.D., Ph.D.

Department of Neurosurgery (HN, TS), Nara Medical University, Nara, Japan, and Institute for Neurosurgical Pathophysiology (OK), Johannes-Gutenberg University Mainz, Mainz, Germany

OBJECTIVE: The application of a laser scanning technique to measure regional cerebral blood flow (CBF) and tissue hemoglobin oxygenation (HbO_2) using the rat closed cranial window preparation is described.

METHODS: Twenty-nine male Wistar rats were used to consecutively measure local CBF by laser Doppler flowmetry and tissue HbO_2 by a microspectrophotometric method at multiple corresponding cortical locations. The scanning technique used a computer-controlled micromanipulator. Data from three experimental models are presented: the whisker stimulation model, the ischemia-reperfusion model, and the sinus-vein thrombosis model. Sequential changes in local CBF and HbO_2 data before, during, and after stimulation, ischemia, and sinus thrombosis were examined. Data from predefined locations within the same region were correlated with the topographical location and then arranged in a three-dimensional image.

RESULTS: In the whisker stimulation model, we found a disproportionate increase in CBF (32 ± 12%) as compared with that of HbO_2 (9 ± 4%) during stimulation. In the ischemia-reperfusion model, the three-dimensional image showed heterogeneous low CBF (depending on the area) and homogeneous HbO_2 at a reduced level during ischemia and postischemic hyperperfusion. However, the range of oxygenation was normal after reperfusion. In the sinus-vein thrombosis model, drainage of the unsaturated blood via the collateral pathways was noted.

CONCLUSION: The laser scanning technique is useful for visualizing sequential changes in hemodynamic-metabolic interactions of cortical brain tissue. This technique can reveal phenomena not detected by traditional monitoring procedures. (Neurosurgery 48:1335–1343, 2001)

Key words: Cerebral blood flow, Laser optical technique, Oxygen metabolism, Rats, Scanning technique

It has been widely accepted that a close regional coupling between cerebral blood flow (CBF) and the tissue metabolic rate is dynamically maintained in the healthy brain; however, it has been reported that stimulus-induced focal augmentation of CBF greatly exceeded the concomitant local increase in the cerebral metabolic rate of oxygen during neural activation by somatosensory stimulation in humans (6). Meanwhile, the disproportionate change in CBF as compared with the cerebral metabolic rate of oxygen was interpreted as an uncoupling of the CBF and oxidative metabolism (i.e., "misery" or "luxury" perfusion). Thus, the relationship remains controversial.

Recently, laser Doppler scanning has became a popular technique for measuring blood flow (4, 9, 12, 20–25). With this technique, the laser Doppler probe is moved to multiple predefined positions in the cranial window by using an exact positioning procedure with a computer-controlled motorized micromanipulator to measure the local CBF (lCBF) in several locations. The data are used to form typical regional CBF (rCBF) histograms and for cortical CBF mapping. The superiority of laser Doppler scanning to conventional single laser Doppler ultrasound has been demonstrated (20–23, 25, 27). The advantages include improved spatial resolution with easy detection of low-flow areas and better comparison of data from individual experiments.

The microspectrophotometric technique provides valuable information for analysis of brain tissue oxygen metabolism, which is related directly to cerebral cortical function. The advantages include the capability of continuous in vivo monitoring with minimal damage to the tissues (3, 7, 8, 19, 28). In this experiment, the laser Doppler scanning technique was expanded by including assessment of tissue hemoglobin oxygenation (HbO_2) from identical locations, a procedure made possible by the similar sampling volumes of both measure-

ment techniques. In this study, we demonstrate that the current technology using a scanning technique permits the in vivo measurement and observation needed to establish a close topographical relationship between lCBF and local HbO_2 ($lHbO_2$).

MATERIALS AND METHODS

Animal preparation

All procedures were carried out in accordance with the animal experiment guidelines approved at the 80th General Assembly of the Japan Science Council in 1980 or the German Animal Protection Legislation. Twenty-nine male Wistar rats, each weighing between 265 and 358 g (mean, 321.9 ± 25.3 g), were premedicated with 0.5 mg of atropine and anesthetized with chloral hydrate (36 mg/100 g) administered intraperitoneally. Anesthesia was maintained with chloral hydrate (12 mg/100 g) administered hourly via a peritoneal catheter. During the experiment, spontaneous ventilation was maintained, and temporal muscle and rectal temperature were maintained at 37°C via a feedback-controlled homeothermic lamp (IFR 100; Unique Medical, Tokyo, Japan) and a blanket control unit (CMA 150; Carnegie Medicine AB, Stockholm, Sweden). Polyethylene catheters were inserted into the right carotid artery or the tail artery and into the right femoral vein. The arterial line served for continuous measurement of the mean arterial blood pressure (MABP) and gas sampling and the venous lines for administration of fluids and drugs. The partial pressure of oxygen in arterial blood, the arterial carbon dioxide pressure, and the arterial pH were measured with a blood gas analyzer (ABL 300 blood gas analyzer; Radiometer, Copenhagen, Denmark). The blood pressure was continuously monitored via an intra-arterial catheter connected to a pressure transducer (polygraph system RM-600; Nihon Kohden, Tokyo, Japan). Each rat was mounted on a stereotactic frame (SR-6; Narishige, Inc., Tokyo, Japan). After a midline skin incision of 1.0 to 2.0 cm, a frontoparietal craniotomy was made with a saline-cooled drill for an area between 3 × 4 mm and 9 × 6 mm with a high-speed drill under an operating microscope (Zeiss, Wetzlar, Germany). Saline of a fixed temperature (37°C) was frequently perfused over the dura during the experiment.

Local CBF and HbO_2 measurement by scanning technique

The lCBF was measured by laser Doppler flowmetry with a 0.8-mm needle probe (ALF-21; Advance, Tokyo, Japan) and expressed in laser Doppler units because the calibration of laser Doppler to absolute flow value units remains controversial. The $lHbO_2$ (in percentage) was measured with a monitor (EMPHO II; Bodenseewerk Geratetechnik GmbH, Uberlingen, Germany). In the monitor, light transmitted by detecting fibers passes a fast rotating interference band-pass filter disc (502–628 nm) and then illuminates a photomultiplier. The raw spectrum thus obtained is corrected on-line with the dark spectrum and with the spectrum obtained from excitation light reflected from a mirror at a set distance (7). The response spectrum is used for evaluation of the tissue spectra from which the $lHbO_2$ is calculated. To do so, the spectra were digitized in increments of 2 nm, ranging from 502 to 628 nm. The relative amounts of oxyhemoglobin and deoxyhemoglobin normalized for light scattering were estimated as parameters with an iterative best-fit procedure based on the theory of Kuberka and Munk (13). These are relative concentrations because of light scattering, although they permit the calculation of the percentage of oxyhemoglobin saturation (7, 13).

Values of lCBF and $lHbO_2$ were measured consecutively at 25 locations (5 × 5) in the whisker stimulation model and the ischemia-reperfusion model and at 48 locations (6 × 8) in the sinus-vein thrombosis model in the parietal cortex. Two probes were used for CBF and HbO_2 measurements. The probes were exchanged with a specially designed probe holder that allows the placement of both probes at identical locations by using the stored coordinates. The scanning procedure was performed via a motor-driven and computer-controlled micromanipulator (xyz scanning stage; Scholar Tec, Osaka, Japan) connected to a 98 Note SX personal computer (NEC, Tokyo, Japan). Thus, the random registration of 25 or 48 individual measurements is produced in one scanning procedure with information from each location with each distance of 400 μm. To avoid artifacts as a result of measurements recorded with a still-moving probe, a delay of 2 seconds was allowed before each measurement. Twenty measurements of CBF measured for the next 2 seconds and 10 measurements of HbO_2 for 1 second were averaged and used as one lCBF and one $lHbO_2$ measurement, respectively. Values of rCBF and regional HbO_2 ($rHbO_2$) were determined by calculating the median value from all locations. This technique permits repeat scanning from a given set of identical locations.

Three-dimensional image

The data collected were used to calculate CBF and HbO_2 for mapping. For cortical mapping, data from multiple locations were expressed as a percentage change from the baseline in the *z* axis. These data were correlated with the topographical location in the cranial window and then arranged for three-dimensional (3-D) images by using xyz triplet columns for a mesh (for CBF) or a scatterplot (for HbO_2) and then interpolated. Illustrations were plotted with SigmaPlot software (Jandel Scientific, Erkrath, Germany).

Animal experimental models

Sham-operated control animals

Five rats served as sham-operated controls and underwent craniotomies only. Both parameters were registered at 25 locations (given anatomic sites) every 15 minutes for a total of 90 minutes.

Whisker stimulation model

In this experiment (Experiment 1), vibrissae stimulation (15, 30) was performed for a period of 3 minutes by continuous manual deflection of all vibrissae on the left side of the rat

face at a frequency of 1 per second. Before, during, and after stimulation, the resting CBF and HbO_2 were monitored in six animals at 25 identical locations over the right somatosensory cortex of the densely innervated whisker hairs located 3 mm caudal and 7 mm lateral to the bregma (15).

Ischemia-reperfusion model

In this experiment (Experiment 2), global ischemia using occlusion of the bilateral carotid arteries coupled with hypobaric hypotension was induced by decreasing the MABP to 40 mm Hg in eight animals. Both carotid arteries were exposed and carefully isolated from the surrounding tissue by using an operating microscope. Special care was taken not to damage the vagus nerve and the peripheral nerve tissue. Polyethylene catheters were inserted into the right carotid artery. The left carotid artery was encircled loosely with 5-0 thread by pulling the carotid snare so that occlusion could be induced later. The lower portion of the body was placed in a negative-pressure chamber connected to an electronically controlled vacuum pump for induction of hypobaric hypotension. The barometric pressure within the chamber could be reduced, and hypotension was caused by pooling of the venous blood in the lower half of the body (5, 23). The MABP was reduced by hypobaric hypotension to 40 mm Hg together with occlusion of the bilateral carotid arteries and maintained constant for 15 minutes. After hypotension and release of the left carotid snare, the experiment was continued for 60 minutes. Values of lCBF and $lHbO_2$ were registered at 25 identical locations before, during, and 15 minutes after ischemia.

Sinus-vein thrombosis model

In this experiment (Experiment 3), sinus-vein thrombosis was induced by ligation using 9-0 Prolene combined with the slow injection of kaolin-cephalin suspension with a 27-gauge needle into the superior sagittal sinus (SSS). The methods used here have been described in detail previously (20). Values of lCBF and $lHbO_2$ were measured at 48 identical locations with a scanning procedure before and after the SSS ligation, after injection of the suspension, and every 15 minutes for a total of 90 minutes after the injection. The animals were operated on in random order, and the data were examined in blinded fashion. The animals were killed and their brains extirpated for histological examination after the experiments.

Statistical analysis

All results are expressed as means ± standard deviations (SD). Values for rCBF and $rHbO_2$ are expressed as the median of lCBF and $lHbO_2$ data, respectively, obtained from all locations. Sequential changes in rCBF and $rHbO_2$ were evaluated by analysis of variance (Dunnett's test) for repeated measurements in all experiments. Statistical significance was assumed at $P < 0.05$. Statistical analysis was performed with SigmaStat software (Jandel Scientific).

RESULTS

Physiological variables

All physiological variables were within the normal limits in all experiments (*Table 1*).

Sham-operated control animals

In the sham-operated control animals, the MABP, rCBF, and $rHbO_2$ were constant during the experiment. The histograms and mapping also revealed no significant changes in CBF or HbO_2 throughout the experiments (data not shown). No histological changes were observed.

Experiment 1: Whisker stimulation model

Stimulation of the whisker stimulation model animals did not affect MABP. The mean rCBF increased from 30 ± 5 to 39 ± 4 laser Doppler units (an increase of 30.8 ± 12%), whereas the mean $rHbO_2$ increased from 56 ± 7% to 60 ± 8% (an increase of 9 ± 4%). After termination of stimulation, both parameters returned to mean baseline levels of 27 ± 5 laser Doppler units and 53 ± 6%, respectively (*Fig. 1A*).

That repeated measurements were performed at multiple locations in each animal allowed the study of changes in CBF and HbO_2 at these sites during the course of the experiment by histograms and 3-D images. The typical lCBF histogram pattern in the control phase was characterized by a left-shifted distribution, with a maximum frequency between 20 and 30 laser Doppler units, and that of HbO_2 was between 40 and 70%. The histograms of both parameters displayed a shift in distribution to the right during whisker barrel stimulation (*Fig. 1B*). On 3-D images, a disproportionate increase in CBF was noted as compared with that in HbO_2 (*Fig. 1C*). No histological changes were observed.

TABLE 1. Data from Arterial Blood Gas Analyses Sampled during the Initial Control Condition Phase of All Experiments[a]

Group	No. of Animals	PO_2 (mm Hg)	PCO_2 (mm Hg)	pH	MABP (mm Hg)
Sham	5	94.3 ± 5.4	43.1 ± 2.3	7.30 ± 0.01	93.0 ± 3.5
Experiment 1	6	93.8 ± 3.1	42.9 ± 1.1	7.32 ± 0.02	92.3 ± 4.7
Experiment 2	8	93.5 ± 6.8	43.2 ± 1.4	7.30 ± 0.02	89.8 ± 6.0
Experiment 3	10	87.1 ± 9.3	46.7 ± 3.2	7.30 ± 0.05	70.4 ± 8.8

[a] **PO_2, partial pressure of oxygen; PCO_2, partial pressure of carbon dioxide; MABP, mean arterial blood pressure. Values are means ± standard deviation.**

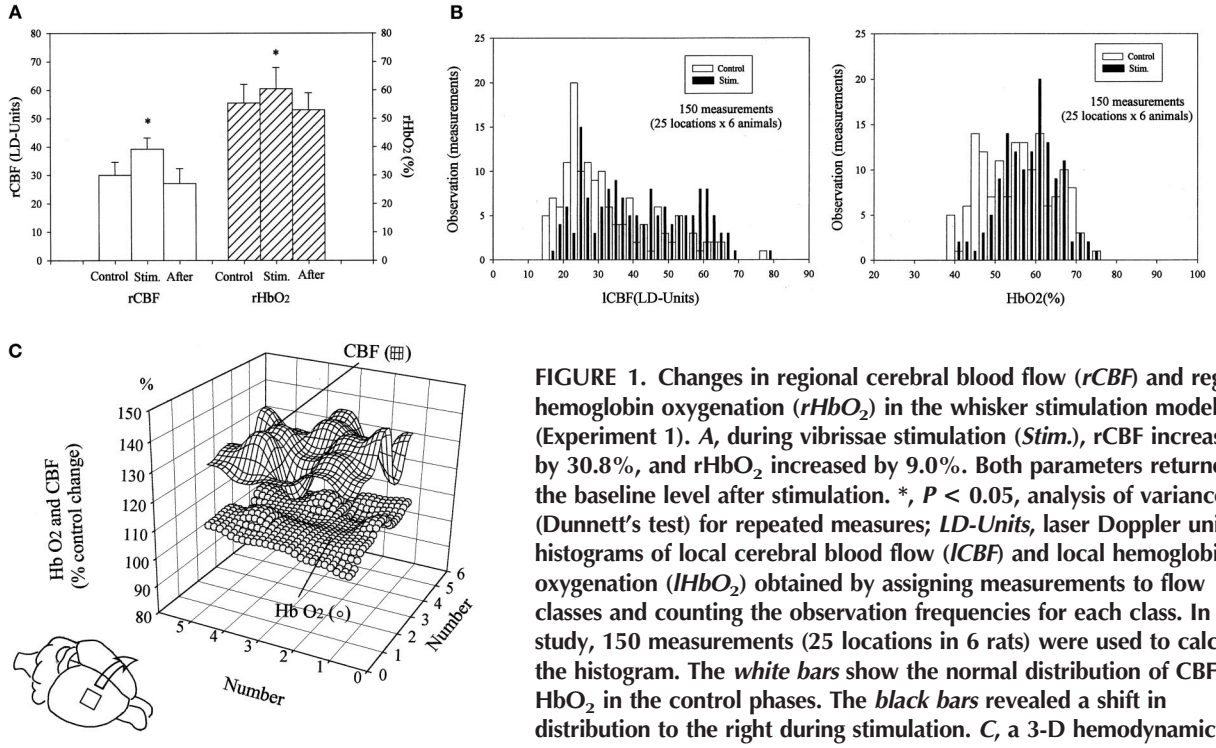

FIGURE 1. Changes in regional cerebral blood flow (*rCBF*) and regional hemoglobin oxygenation ($rHbO_2$) in the whisker stimulation model (Experiment 1). *A*, during vibrissae stimulation (*Stim.*), rCBF increased by 30.8%, and $rHbO_2$ increased by 9.0%. Both parameters returned to the baseline level after stimulation. *, $P < 0.05$, analysis of variance (Dunnett's test) for repeated measures; *LD-Units*, laser Doppler units. *B*, histograms of local cerebral blood flow (*lCBF*) and local hemoglobin oxygenation ($lHbO_2$) obtained by assigning measurements to flow classes and counting the observation frequencies for each class. In this study, 150 measurements (25 locations in 6 rats) were used to calculate the histogram. The *white bars* show the normal distribution of CBF and HbO_2 in the control phases. The *black bars* revealed a shift in distribution to the right during stimulation. *C*, a 3-D hemodynamic-metabolic image of a typical experiment displaying a disproportionate increase in cerebral blood flow (*CBF*) as compared with that of HbO_2. The data are expressed as a percentage of the baseline value found at each location.

Experiment 2: Ischemia-reperfusion model

In the ischemia-reperfusion model, animals at an MABP of 90 ± 6 mm Hg, the mean control values for rCBF and $rHbO_2$ were 20 ± 5 laser Doppler units and 53 ± 6%, respectively. At an MABP of 40 mm Hg, together with occlusion of the bilateral carotid arteries, rCBF and $rHbO_2$ dropped significantly to 8 ± 4 laser Doppler units ($P < 0.05$ versus the control) and 27 ± 12% ($P < 0.05$ versus the control) in the beginning of ischemia (*Fig. 2A*). The MABP further decreased to 6 ± 3 laser Doppler units ($P < 0.05$) and 17 ± 7% ($P < 0.05$) at the end of ischemia (*Fig. 2A*). After hypotension and release of the left carotid snare, values for MABP, rCBF, and $rHbO_2$ recovered sharply to the original level. The levels of MABP and $rHbO_2$ were maintained until the end of the experiment, whereas rCBF was increased significantly at 30 minutes (35 ± 12 laser Doppler units) and at 45 minutes (35 ± 14 laser Doppler units) after induced ischemia ($P < 0.05$)(*Fig. 2A*).

At the beginning of ischemia, 3-D images demonstrated a heterogeneous low CBF (depending on the area) and homogeneous (slightly low) level of HbO_2 (*Fig. 2B*). At the end of ischemia, both parameters were severely reduced (*Fig. 2C*). After ischemia, 3-D images demonstrated hyperperfusion and a normal range of oxygenation (*Fig. 2D*). Histologically, significant neuronal losses were observed.

Experiment 3: Sinus-vein thrombosis model

Thrombosis of SSS and cortical veins, a decrease in rCBF, and a decrease in tissue HbO_2 and brain damage (bilateral parasagittal infarction) were observed in 10 of the 18 experimental rats (20). No significant changes were noted in the remaining eight animals. A reduction in tissue HbO_2 preceded the decrease in flow. 3-D images demonstrated no change in CBF and a widespread decline in HbO_2 along the cortical vein immediately after sinus ligation, especially at the distal side of the cortical vein (distant from the SSS) (*Fig. 3A*); both parameters further decreased after injection of kaolin-cephalin suspension and continued to decrease with progression of thrombosis below the ischemic threshold (*Fig. 3B*).

DISCUSSION

A scanning laser optical technique

Although conventional (stationary) laser Doppler ultrasound allows noninvasive and continuous recording of the actual time course of CBF (5), it has ill-defined resolution (1–2 mm^3), is of limited utility in the evaluation of absolute CBF, and is highly dependent on localization of the laser Doppler probe and the underlying anatomic substrate. The laser Doppler scanning system has been developed to overcome the limitations of laser Doppler flowmetry. The technique permits the estimation of rCBF from local measurements (9, 12, 20–23, 25). The number of measurements necessary to assess rCBF by lCBF recording has been evaluated in a recent simulation study using the scanning technique, and a sample size of greater than 25 is necessary to obtain reliable information regarding rCBF (12). Accordingly, a sampling size of more

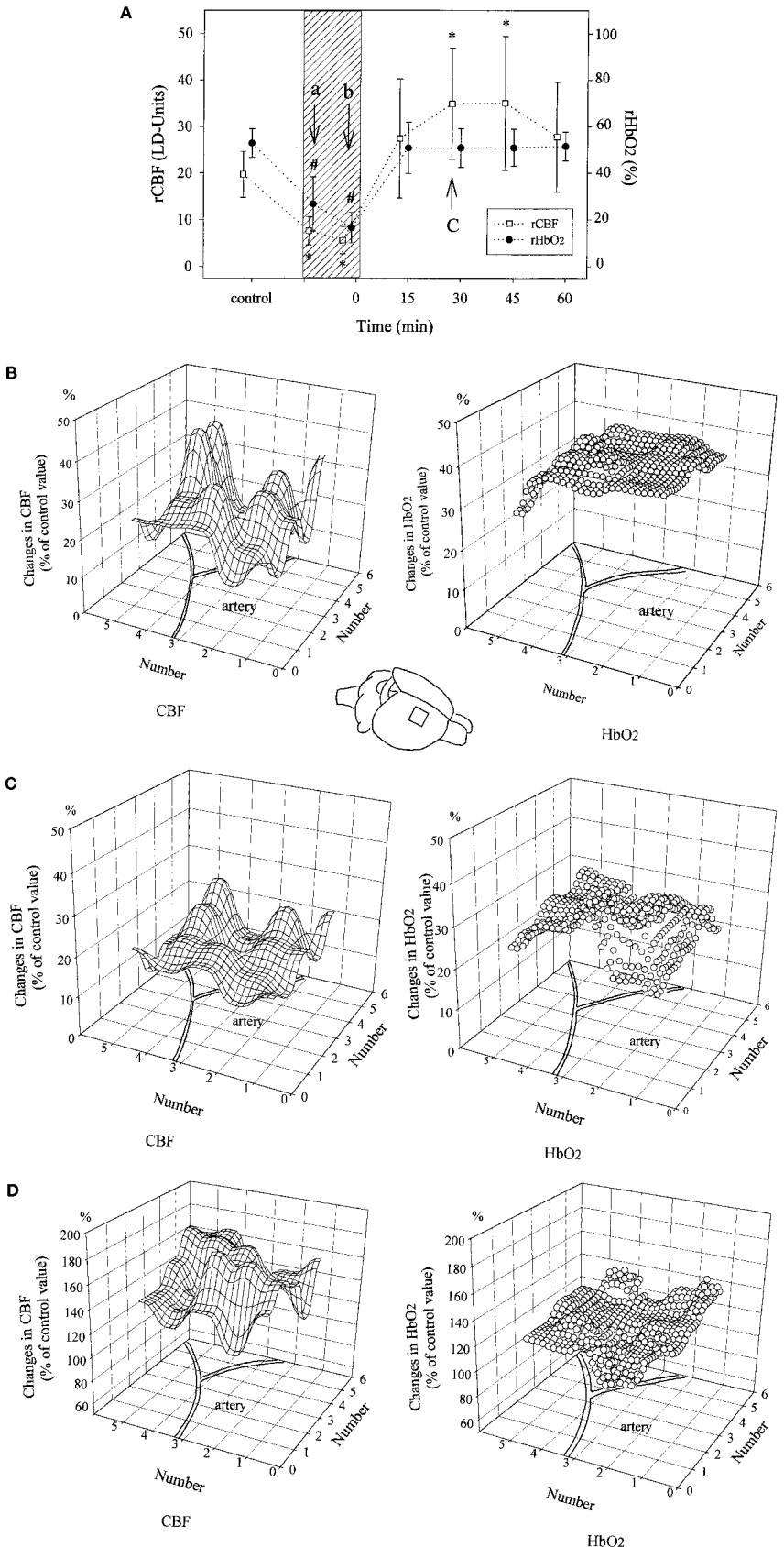

FIGURE 2. Sequential changes in regional cerebral blood flow (*rCBF*) and regional hemoglobin oxygenation ($rHbO_2$) in the ischemia-reperfusion model (Experiment 2). *A*, changes in rCBF and $rHbO_2$, expressed as laser Doppler units (*LD-Units*) and percentages at the beginning of ischemia (*a*), at the end of ischemia (*b*), and 30 minutes after ischemia (*C*). Values are mean ± SD. # and *, $P < 0.05$, analysis of variance (Dunnett's test) for repeated measures. The *hatched bar* indicates induced hypotension coupled with occlusion of the bilateral carotid arteries. *B*, 3-D images at the beginning of ischemia (*a* in *A*) in a typical experiment showing a heterogeneous cerebral blood flow (*CBF*) depending on the area and existence of stabilized oxygenated hemoglobin (HbO_2). Note that the area remote from the artery (the low-flow zone) sustained a severe reduction in CBF but a mild decline in HbO_2. *C*, 3-D images at the end of ischemia (*b* in *A*) in the same rat showing a severe reduction of both parameters. *D*, 3-D images at 30 minutes after ischemia (*C* in *A*) demonstrating postischemic hyperperfusion but a normal range of oxygenation.

than 25 was used in the present study. The ability of the micromanipulator to precisely return to a given location over the cortex has been reported, and the accuracy of repeated scans with the use of the micromanipulator has been excellent (9, 25). Regarding the effect of the superficial arteries and veins, the rCBF changes could be analyzed by creating frequency histograms exhibiting a nongaussian distribution in the scanning technique. The histograms displayed a typical pattern, depending on the vessel architecture of the species examined. In addition, 3-D mapping demonstrated microcirculatory changes and the presence of the superficial arteries and veins. We have already performed validation studies of these techniques: a linear relationship between laser Doppler scanning (laser Doppler units) and hydrogen clearance (ml/100 g/min) (27), and a relationship between tissue HbO_2 scanning (%) and tissue partial pressure of oxygen (mm Hg) (24).

The microspectrophotometric technique provided valuable information for

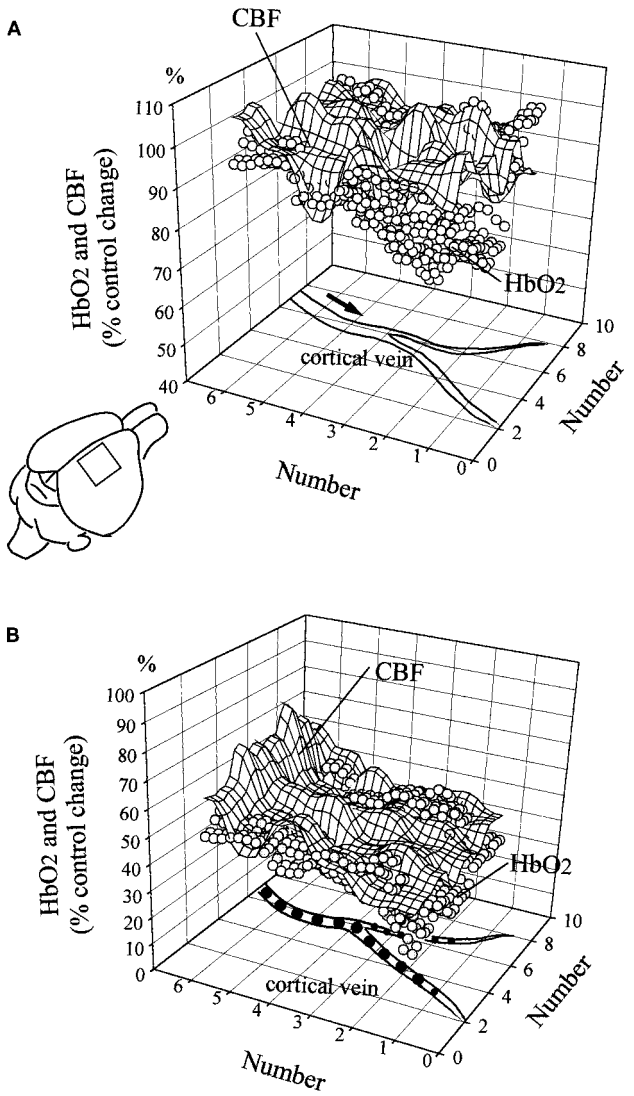

FIGURE 3. 3-D images of rCBF and oxygenated hemoglobin (*HbO_2*) in the sinus-thrombosis model (Experiment 3). *A*, after sinus ligation in the typical experiment showing a slight decrease in cerebral blood flow (*CBF*) and widespread decline in HbO_2 along the cortical vein. In particular, in the area distal from the SSS, HbO_2 decreased more than CBF. The *black arrow* points to a reverse flow in the cortical vein, which is detected by angiography. *B*, at 90 minutes after SSS occlusion in the same rat revealing that lCBF and $lHbO_2$ were reduced diffusely and were below the ischemic threshold at many locations. Thrombus is indicated by *black dots*, and the cortical vein was thrombosed almost completely.

the investigation of brain tissue oxygen metabolism. Williams et al. (29) monitored the intracerebral HbO_2 in patients undergoing carotid endarterectomy by near-infrared spectroscopy, which detected cerebral hypoxia in association with episodes of hypotension. Thus, cerebral oximetry is expected to be used with increasing frequency as a reliable method for monitoring early cerebral hypoxia. In the current experiment, a scanning system was applied to both laser Doppler scanning and microspectrophotometric techniques for measuring the lCBF and $lHbO_2$ of multiple locations with the use of needle probes.

Whisker stimulation model

The advantage of the whisker barrel model for investigation of the coupling of CBF, metabolism, and neuronal function is the physiological stimulation mode (10, 15). This study demonstrated that CBF and HbO_2 increased entirely in the barrel area, but the CBF increases incurred during stimulation of the neuronal activity were disproportionally high (approximately 30%) as compared with the change in the metabolic rate of oxygen (nearly 9%). The differences are considered to demonstrate the relationship between supply and demand in oxygen metabolism. The current observation is in agreement with those of other reports (6).

Ischemia-reperfusion model

The dynamics of regional pathophysiological changes after transient ischemic insult are still ill defined, inasmuch as repeated measurements of several physiological variables such as CBF and oxygenation cannot be performed easily with the standard experimental procedures. The methodology used here permits repetitive flow and oxygen metabolic measurement (*Fig. 2A*). At the beginning of ischemia, the 3-D images demonstrated the so-called misery-perfusion syndrome (2), most likely a result of an increase in oxygen extraction fraction against the decline of CBF (*Fig. 2B*). At the end of ischemia, the images showed the condition of "penumbra" (1) and below the ischemic threshold (*Fig. 2C*). In the penumbra state, the cells are alive but the metabolic pumps are inhibited and oxidative metabolism is reduced. At 30 minutes after ischemia, the images showed postrecanalization hyperperfusion ("luxury perfusion") (14), which has been associated with both a good prognosis (18) and a poor prognosis (11) (*Fig. 2D*). In the reperfusion phase, excessive oxygen consumption in the brain may occur as a result of a seizurelike condition such as reperfusion-induced arrhythmia observed in the heart (17).

Sinus-vein thrombosis model

In an earlier study (20), we reported that CBF, tissue HbO_2, and findings of repeated angiography can be useful markers for the early detection of critical conditions after sinus-vein thrombosis and found that a reduction in tissue HbO_2 preceded the flow decrease. The 3-D image demonstrated a widespread decline in HbO_2 along the occluded vein that was related to drainage of the desaturated blood via complex collateral pathways (*Fig. 3A*). This finding is an incentive for earlier detection of critical cerebral venous circulation disorders with HbO_2 than with CBF monitoring. Because the individual availability of collateral vessels in cerebral venous circulation disorders seemed to determine the outcome (22), tissue HbO_2 monitoring may be the most useful method of detecting dangerous venous circulation disturbance at an early stage.

3-D hemodynamic and oxygen metabolic imaging

In this study, we used a 3-D alignment procedure using data on CBF and HbO_2 obtained from scanning and found that the 3-D image permitted in vivo observation and consequently established a close topographical relationship between CBF and oxidative metabolism by careful semiquantitative assessment. As compared with other optical imaging techniques (10, 16) and functional magnetic resonance imaging (26), laser Doppler scanning can provide hemodynamic-metabolic imaging and statistical analysis. This method particularly suits studies in the area in which lCBF and $lHbO_2$ heterogeneities are expected and can provide close evaluation of individual experiments. Some phenomena cannot be detected solely by calculation of these parameters, and therefore the topographical image is informative (as shown in *Fig. 3A*). This technique can reveal phenomena previously undetected by conventional methods, and must enhance the value of in vivo visualization of the brain.

CONCLUSIONS

The scanning laser optical technique is a promising new technique for in vivo measurement and observation of the hemodynamic-metabolic interrelationship in the brain and will lead to a better understanding of cerebral microcirculation and oxidative metabolism under pathological and the physiological conditions in individual experimental animals.

ACKNOWLEDGMENTS

This study was supported in part by a Grant-in-Aid for Scientific Research B-2 (No. 07457321) from the Japan Ministry of Education, Science, Sports and Culture. We thank Kaori Fuchigami for technical assistance in the animal experiments and Mieko Onoue for excellent editorial assistance.

Received, July 19, 2000.
Accepted, January 22, 2001.
Reprint requests: Hiroyuki Nakase, M.D., Department of Neurosurgery, Nara Medical University, 840 Shijo-cho, Kashihara, Nara 634-8522, Japan. Email: nakasehi@nmu-gw.naramed-u.ac.jp

REFERENCES

1. Astrup J, Siesjo BK, Symon L: Thresholds in cerebral ischemia: The ischemic penumbra. **Stroke** 12:723–725, 1981.
2. Baron JC, Bousser MG, Rey A, Guillard A, Comar D, Castaigne P: Reversal of focal "misery-perfusion syndrome" by extra-intracranial arterial bypass in hemodynamic cerebral ischemia. **Stroke** 12:454–459, 1981.
3. Beck T, Krieglstein J: Cerebral circulation, metabolism, and blood-brain barrier of rats in hypocapnic hypoxia. **Am J Physiol** 252: H504–H512, 1987.
4. Dirnagl U, Kaplan B, Jacewicz M, Pulsinelli W: Continuous measurement of cerebral blood flow by laser-Doppler flowmetry in a rat stroke model. **J Cereb Blood Flow Metab** 9:589–596, 1989.
5. Dirnagl U, Thoren P, Villringer A, Sixt G, Them A, Einhaupl KM: Global forebrain ischemia in the rat: Controlled reduction of cerebral blood flow by hypotension and two-vessel occlusion. **Neurol Res** 15:128–130, 1993.
6. Fox PT, Raichle ME: Focal physiological uncoupling of cerebral blood flow and oxidative metabolism during somatosensory stimulation in human subjects. **Proc Natl Acad Sci U S A** 83:1140–1144, 1986.
7. Frank K, Funk R, Kessler M, Rohen JW: Spectrometric measurement in the anterior eye vasculature of the albino rabbit: A study with the EMPHO I. **Exp Eye Res** 52:301–309, 1991.
8. Friedland RP, Iadecola C: A centennial reexamination of "On the regulation of the blood-supply of the brain." **Neurology** 41:10–14, 1991.
9. Heimann A, Kroppenstedt S, Ulrich P, Kempski OS: Cerebral blood flow autoregulation during hypobaric hypotension assessed by laser Doppler scanning. **J Cereb Blood Flow Metab** 14:1100–1105, 1994.
10. Hodge CJ, Stevens RT, Newman H, Merola J, Chu C: Identification of functioning cortex using cortical optical imaging. **Neurosurgery** 41:1137–1145, 1997.
11. Infeld B, Davis SM, Donnan GA, Lichtenstein M, Baird AE, Binns D, Mitchell PJ, Hopper JL: Streptokinase increases luxury perfusion after stroke. **Stroke** 27:1524–1529, 1996.
12. Kempski O, Heimann A, Strecker U: On the number of measurements necessary to assess regional cerebral blood flow by local laser Doppler recordings: A simulation study with data from 45 rabbits. **Int J Microcirc Clin Exp** 15:37–42, 1995.
13. Kuberka P, Munk F: Ein Beitrag zur Optik der Farbanstriche. **Z Technische Physik** 11a:76–77, 1930.
14. Lassen NA: The luxury-perfusion syndrome and its possible relation to acute metabolic acidosis localized within the brain. **Lancet** 2:1113–1115, 1966.
15. Lindauer U, Villringer A, Dirnagl U: Characterization of CBF response to somatosensory stimulation: Model and influence of anesthetics. **Am J Physiol** 264:H1223–H1228, 1993.
16. Malonek D, Tootell RB, Grinvald A: Optical imaging reveals the functional architecture of neurons processing shape and motion in owl monkey area MT. **Proc R Soc Lond [Biol]** 258:109–119, 1994.
17. Manning AS, Hearse DJ: Reperfusion induced arrhythmias: Mechanisms and prevention. **J Mol Cell Cardiol** 16:497–518, 1984.
18. Marchal G, Furlan M, Beaudouin V, Rioux P, Hauttenment JL, Serrati C, de-la-Sayette V, Le-Doze F, Viader F, Derlon JM, Baron JC: Early spontaneous hyperperfusion after stroke: A maker of favorable tissue outcome? **Brain** 119:409–419, 1996.
19. McCormick PW, Stewart M, Goetting MG, Balakrishnan G: Regional cerebrovascular oxygen saturation measured by optical spectroscopy in humans. **Stroke** 22:596–602, 1991.
20. Nakase H, Heimann A, Kempski O: Alterations of regional cerebral blood flow and tissue oxygen saturation in a rat sinus-vein thrombosis model. **Stroke** 27:720–727, 1996.
21. Nakase H, Heimann A, Kempski O: Local cerebral blood flow in a rat cortical vein occlusion model. **J Cereb Blood Flow Metab** 16:720–728, 1996.
22. Nakase H, Kempski O, Heimann A, Takeshima T, Tintera J: Microcirculation after cerebral venous occlusion as assessed by laser Doppler scanning. **J Neurosurg** 87:307–314, 1997.
23. Nakase H, Nagata K, Otsuka H, Sakaki T, Kempski O: Local cerebral blood flow autoregulation following asymptomatic cerebral venous occlusion in the rat. **J Neurosurg** 89:118–124, 1998.
24. Nakase H, Ohtsuka H, Uranishi R, Kotani A, Kaido T, Sakaki T: Evaluation of absolute oxygenation of tissue $HbSO_2$-scanning: Comparison with tissue PO_2 [in Japanese]. **Jpn J Cereb Blood Flow Metab** 12:231–232, 2000.

25. Nakase H, Takeshima T, Miyamoto K, Uranishi R, Sakaki T: Cerebral blood flow changes corresponding with arterial blood pressure reduction assessed by laser-Doppler scanning [in Japanese]. **Jpn J Cereb Blood Flow Metab** 9:18–25, 1997.
26. Silva AC, Lee SP, Yang G, Iadecola C, Kim SG: Simultaneous blood oxygenation level-dependent and cerebral blood flow functional magnetic resonance imaging during forepaw stimulation in the rat. **J Cereb Blood Flow Metab** 19:871–879, 1999.
27. Uranishi R, Nakase H, Sakaki T, Kempski O: Evaluation of absolute cerebral blood flow by laser-Doppler scanning: Comparison with hydrogen clearance. **J Vasc Res** 36:100–105, 1999.
28. Wei HM, Chen WY, Sinha AK, Weiss HR: Effect of cervical sympathectomy and hypoxia on the heterogeneity of O_2 saturation of small cerebrocortical veins. **J Cereb Blood Flow Metab** 13:269–275, 1993.
29. Williams IM, Picton AJ, Hardy SC, Mortimer AJ, McCollum CN: Cerebral hypoxia detected by near infrared spectroscopy. **Anaesthesia** 49:726–766, 1994.
30. Woolsey TA, Loos H: The structural organization of layer in the somatosensory region (SI) of mouse cerebral cortex. **Brain Res** 17:205–242, 1970.

COMMENTS

This article by Nakase et al. presents a combination of techniques to allow the simultaneous examination of regional cerebral blood flow (rCBF) and tissue hemoglobin oxygenation (HbO_2) over a region of the cortex. Essential to this study is a computer-controlled micromanipulator with the ability to place separate probes in an identical spot to obtain physiological data. By simultaneously examining flow and tissue oxygenation, the authors examined models of cortical change and suggested possible applications to other clinical conditions and eventually to human conditions.

In this study, whisker stimulation, ischemia with reperfusion, and sinus vein-thrombosis models were examined. Of particular interest are those conditions in which a mismatch between oxygenation and perfusion in response to cortical activation may be possible. Physiological stimulation, for example, increased flow beyond that of metabolism, suggesting that a close linkage of metabolites in the flow may vary according to the conditions. In the ischemia model, "misery perfusion" syndrome was initially observed, but with reperfusion, the authors suggest an increased cerebral blood flow (CBF) with normal HbO_2, a "luxury perfusion" state. The sinus-vein thrombosis model demonstrated that metabolic changes preceded flow changes because of collateral. These findings, although not exceptionally surprising in themselves, suggest considerable applications for this modality of testing in other models of ischemia, cortical dysfunction, or metabolic demand. Whether the procedure could become acceptable in the clinical laboratory of the intensive care unit in the future needs to be examined. We look forward to the implications of such simultaneous monitoring.

Robert J. Dempsey
Madison, Wisconsin

The authors describe and demonstrate a novel technique that allows an estimation of relative blood flow and simultaneous oxygenation in a precise spatial array. This technique allows for the study of metabolic rCBF relationships in a variety of physiological and pathological situations and thus provides a better understanding of the linkage between neuronal activity, blood flow, and oxygen use. The technique described in this article contains various time limitations that mask the occurrence of some important early events in response to neuronal activation. For instance, it is well recognized that an early decrease in local oxygen saturation with neuronal activation is likely to trigger later vasodilation and a resultant increase in rCBF and oversupply of HbO_2 (1). The initial decrease in oxygen saturation is a better indicator of the location of neuronal activity than the later increase in oxygenation. Nonetheless, for experiments that do not require the identification of these initial phases of activity, the technique described in this article has potential value.

Charles J. Hodge, Jr.
Syracuse, New York

---

1. Frostig RD, Lieke EE, Ts'o DY, Grinvald A: Cortical functional architecture and local coupling between neuronal activity and the microcirculation revealed by in vivo high-resolution optical imaging of intrinsic signals. **Proc Natl Acad Sci U S A** 87:6082–6086, 1990.

Nakase et al. have developed a system to measure changes in rCBF repeatedly and in different brain areas by using laser Doppler scanning flowmetry and to simultaneously estimate tissue HbO_2 in the same areas. Although both techniques are indirect measures of the intended end points, the authors have reported other studies showing good correlations between values obtained by these methods and actual CBF measured by hydrogen clearance and tissue oxygen content. Furthermore, many of the artifacts and sources of error in both techniques may be minimized when recordings are performed in a single session and when percentage changes from baseline are used rather than absolute values. Previously, the authors reported that cerebral oxygen saturation declined before CBF in a rat model of sinus thrombosis (2). This was postulated to be a result of the greater sensitivity of hemoglobin saturation to flow reversal and decreased flow velocities in the microcirculation, leading to hemoglobin desaturation before actual reduction in blood flow. The present findings confirm this. In addition, the authors demonstrate that the technique can be used to monitor misery and luxury perfusion in an ischemia-reperfusion model. The authors also demonstrate that whisker stimulation is associated with a 9% increase in hemoglobin saturation and a 30% increase in CBF in the appropriate area of brain.

Other techniques have been used to study the coupling of CBF and neuronal activation in the brains of animals and humans, and similar conclusions have been reached (4). Positron emission tomography can be used to measure CBF, oxygen metabolism, and blood volume, although the temporal and spatial resolution is limited and the technology needed to perform the measurements is not widely available. Controversy exists regarding what is actually measured by functional magnetic resonance imaging (fMRI), but it has been suggested that in blood oxygenation level-dependent (BOLD) fMRI, changes are detected in the concentration of deoxyhemoglobin and in cerebral blood volume.

Silva et al. (4) reported spatial resolution of 470 μm in rats imaged with BOLD fMRI with a 9.4-tesla magnet. Optical imaging measures color changes associated with alterations in cerebral blood oxygen content or blood volume with very high resolution (<200 μm). Nakase et al. add to a body of literature studying the temporal and spatial relationship between altered neuronal activity and CBF. Their technique has the advantage of measuring blood flow and tissue HbO_2 with high spatial resolution over relatively large areas of the brain. Malonek et al. (1) used imaging spectroscopy and laser Doppler flowmetry to study the temporal relationship between neuronal activity in the optic cortex of cats in response to sensory stimulation and blood flow. Spectroscopy measured total and oxygenated hemoglobin with a spatial resolution of 200 μm. The system had a temporal resolution of milliseconds, which is an advantage over the system that Nakase et al describe. The earliest change observed was an increase in deoxyhemoglobin. The increase in CBF followed this by more than a second. The initial increase in deoxyhemoglobin was accompanied by an increase in total hemoglobin, which was postulated to be a result of increased cerebral blood volume. The results were consistent with regulation of cerebral blood volume at a capillary level and with the idea that the initial neuronal activation causes a very localized increase in deoxyhemoglobin, with the secondary increase in CBF being more diffuse. The reverse was reported in studies using BOLD fMRI, which is a source of some controversy in the field (3). It seems likely that advances in imaging techniques will continue to increase the temporal and spatial resolution of these techniques and will lead to a method of noninvasive assessment. The system presented in this article seems to be an advance in this area of inquiry.

R. Loch Macdonald
Chicago, Illinois

1. Malonek D, Dirnagl U, Lindauer U, Yamada K, Kanno I, Grinvald A: Vascular imprints of neuronal activity: Relationships between the dynamics of cortical blood flow, oxygenation, and volume changes following sensory stimulation. **Proc Natl Acad Sci U S A** 94:14826–14831, 1997.
2. Nakase H, Heimann A, Kempski O: Alterations of regional cerebral blood flow and oxygen saturation in a rat sinus-vein thrombosis model. **Stroke** 27:720–728, 1996.
3. Silva AC, Lee SP, Iadecola C, Kim SG: Early temporal characteristics of cerebral blood flow and deoxyhemoglobin changes during somatosensory stimulation. **J Cereb Blood Flow Metab** 20:201–206, 2000.
4. Silva AC, Lee SP, Yang G, Iadecola C, Kim SG: Simultaneous blood oxygenation level-dependent and cerebral blood flow functional magnetic resonance imaging during forepaw stimulation in the rat. **J Cereb Blood Flow Metab** 19:871–879, 1999.

This well-executed experimental study in rats tested the possibilities of a laser scanning technique to analyze and compared the changes in local CBF (lCBF) resulting in rCBF with oxygen metabolism (oxyhemoglobin level) in different physiological and pathological situations. The whisker stimulation, the ischemia-reperfusion, and the sinus-thrombosis models were studied, with the ischemia-reperfusion and the sinus-thrombosis models being well suited for clinical applications. A three-dimensional alignment procedure successfully demonstrated the topographical differences between CBF and oxidative metabolism.

Basic measurements in steady-state condition revealed rather constant values. Physiological stimulation increased flow by 30%, but oxygen metabolism increased flow by only 9%; the flow therefore did not follow the demands of the metabolism. In the ischemia model, produced by hypobaric hypotension and a total of 15 minutes of cerebral ischemia, the regional CBF was heterogeneously low; at the same time, HbO_2 first was in a state that the authors called the misery perfusion syndrome. Increased ischemia simulated penumbra with metabolism below the ischemic threshold. Reperfusion produced an increased CBF with normal HbO_2, the luxury perfusion syndrome. The sinus-vein thrombosis model demonstrated that HbO_2 decreased before the flow changed. This was explained by the possible venous collateral pathways. HbO_2 monitoring is obviously suitable for venous circulation disturbances.

The theoretical models worked very well in this experimental setup and are suited for further experimental evaluation of the complicated pathophysiology of brain ischemia. Clinical applications will be available in the near future, especially in monitoring devices for cerebral ischemia in vascular surgery.

Matti Vapalahti
Kuopio, Finland